

Influence of grain boundary mobility on microstructure evolution during recrystallization

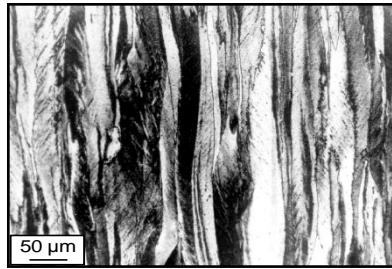
Myrjam Winning, Dierk Raabe



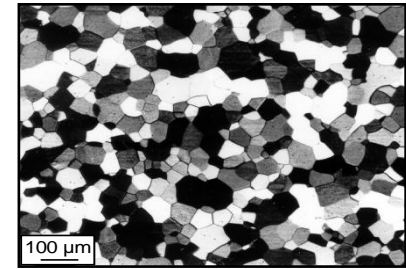
Max-Planck-Institut
für Eisenforschung GmbH
Düsseldorf, Germany

WWW.MPIE.DE
m.wining@mpie.de,
d.raabe@mpie.de

We would like to thank the Deutsche Forschungsgemeinschaft for financial support through the Heisenberg program (Wi 1917/4-1).



deformed



recrystallized

- Recrystallization: change of microstructure as well as of the properties of crystalline materials.
- Experimental evidence for influence of low angle grain boundaries, but they are usually not taken into account.
- Recrystallization models discriminate between three different types of grain boundaries.
- Only few simulations investigated the effect of different grain boundary mobilities on the recrystallization behavior, but without taken into account a non-zero low angle grain boundary mobility.



Investigation whether there is any influence of low angle grain boundaries on the microstructure and texture evolution during recrystallization.

- Attribute of each cell: orientation, dislocation density
- State: „recrystallized“ or „non-recrystallized“
- Switching rule: probabilistic formulation of the Turnbull equation

- Turnbull equation:

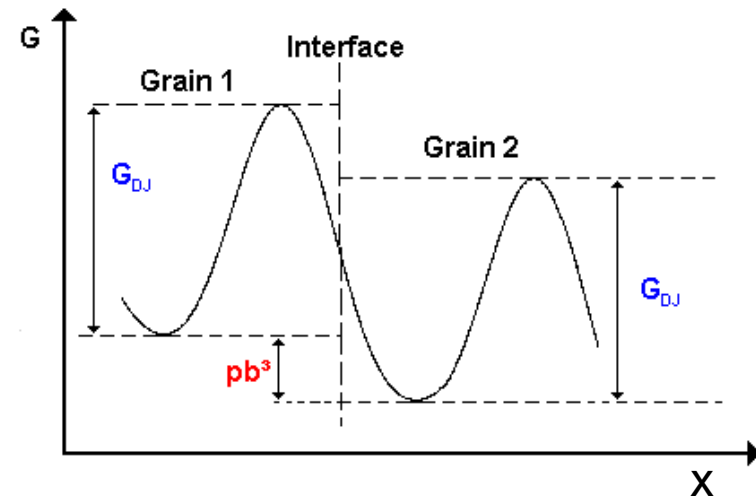
$$v = mp = m_0 \exp(-Q/kT) p$$

- New formulation with two contributions:

$$v = v_0 w$$

$$\text{Deterministic part: } v_0 = \frac{kTm_0}{b^3}$$

$$\text{Probabilistic part: } w = \frac{pb^3}{kT} \cdot \exp\left(-\frac{Q}{kT}\right)$$





- simulation box 100x100x100 cells with $1 \times 1 \times 1 \mu\text{m}^3$ cell size
- Al single crystal with Cube orientation
- nucleation takes place site saturated and randomly at $t = 0$
- driving force results only from difference in stored energy
- constant dislocation density

Case 1:

Case 2:

Case 3:

HAGB: $\Delta H = 1.6 \text{ eV}$ and $m_0 = 1.45 \times 10^{12} \mu\text{m/sMPa}$

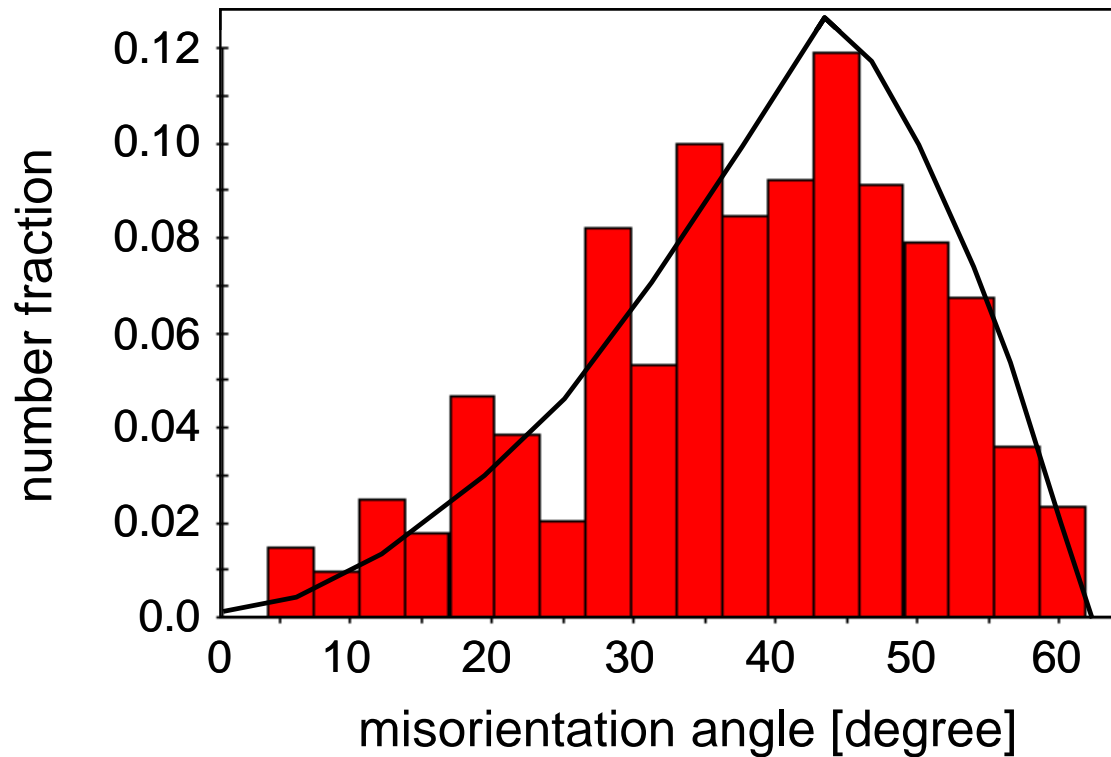
HAGB: $\Delta H = 1.6 \text{ eV}$ and $m_0 = 1.45 \times 10^{12} \mu\text{m/sMPa}$

HAGB: $\Delta H = 1.0 \text{ eV}$ and $m_0 = 7.78 \times 10^8 \mu\text{m/sMPa}$

LAGB: $m = 0$

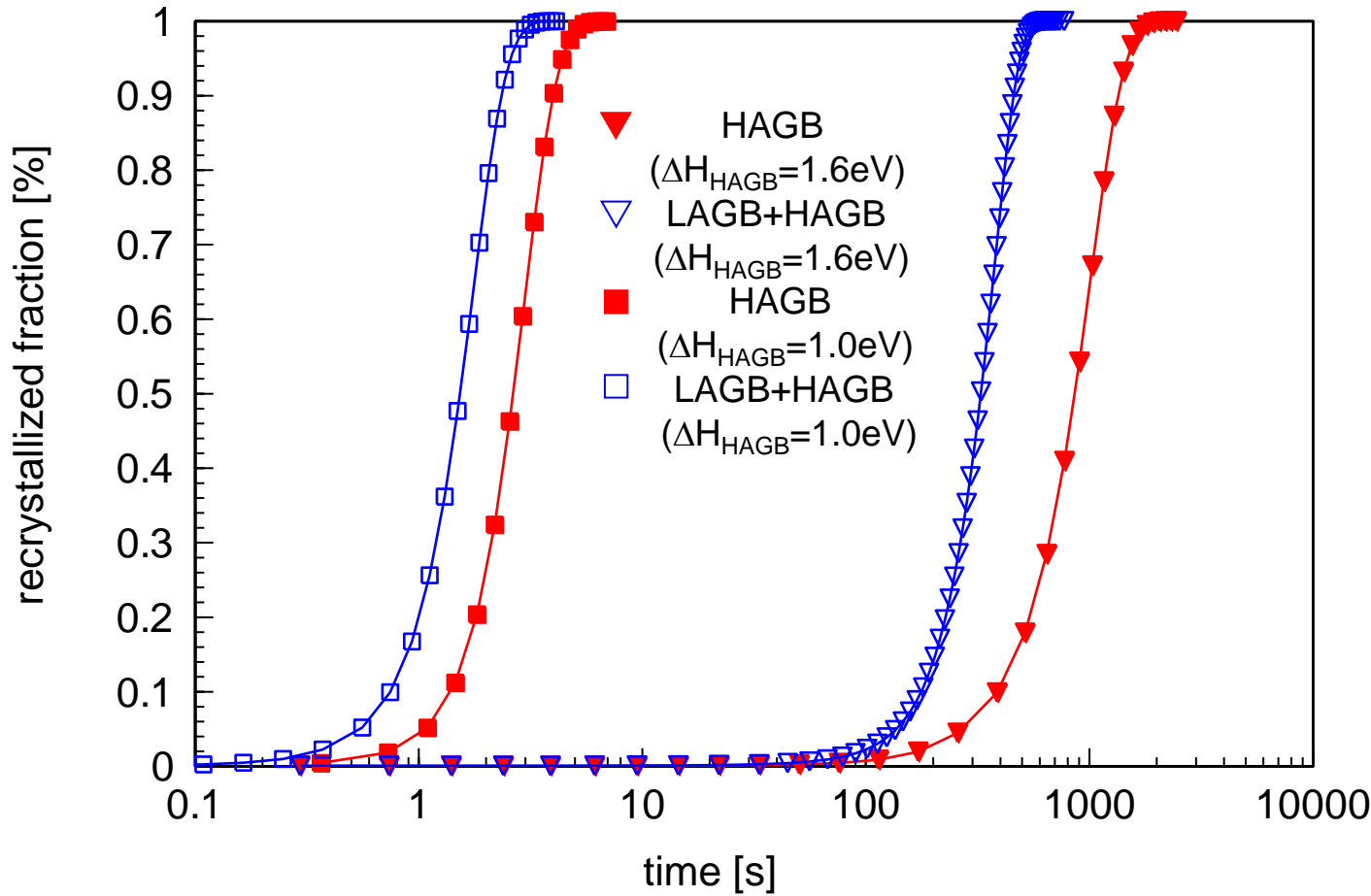
LAGB: $\Delta H = 1.3 \text{ eV}$ and $m_0 = 2.65 \times 10^{10} \mu\text{m/sMPa}$

LAGB: $\Delta H = 1.3 \text{ eV}$ and $m_0 = 2.65 \times 10^{10} \mu\text{m/sMPa}$

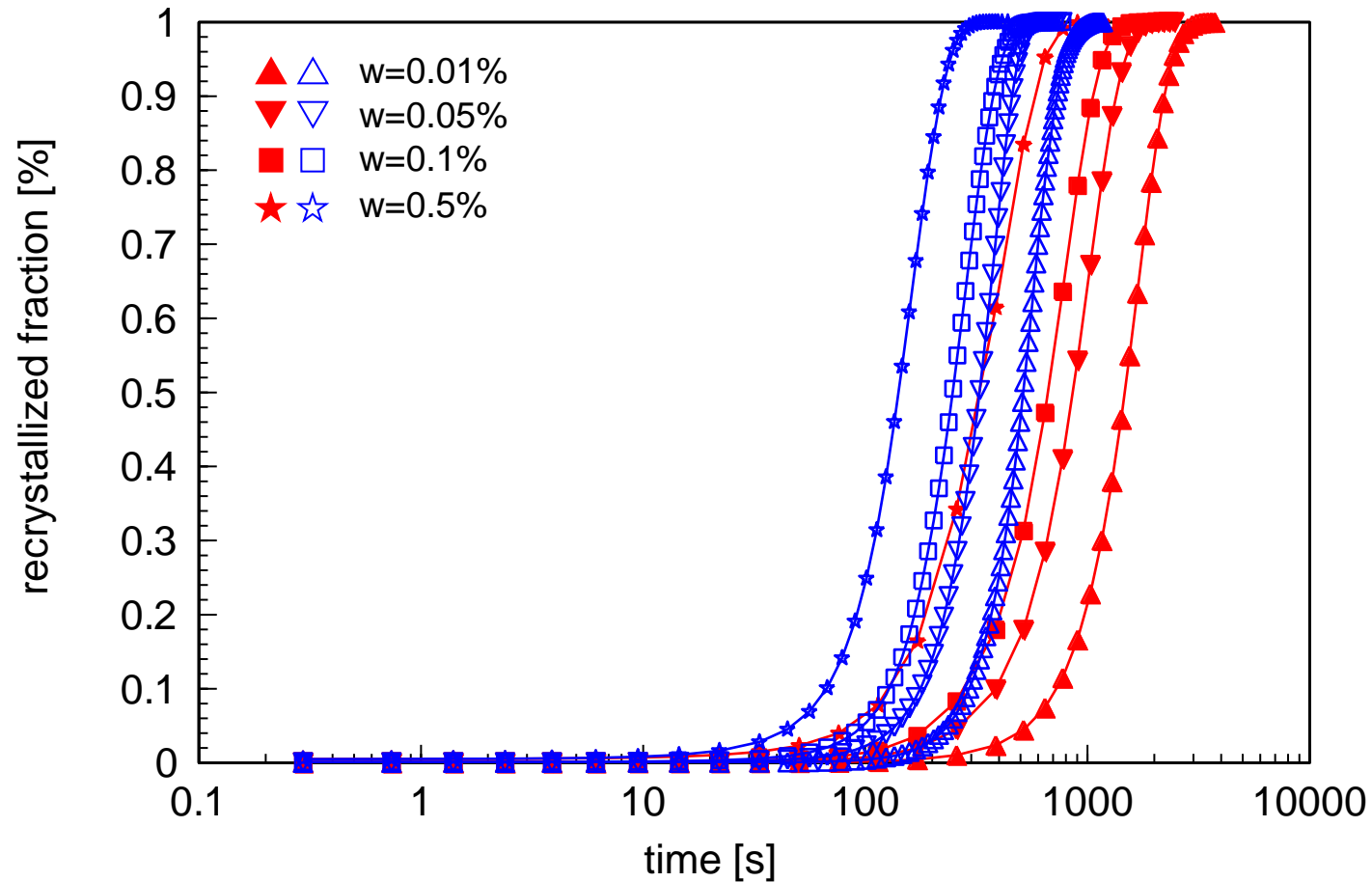


Nucleus distribution very similar for case 1, case 2 and case 3

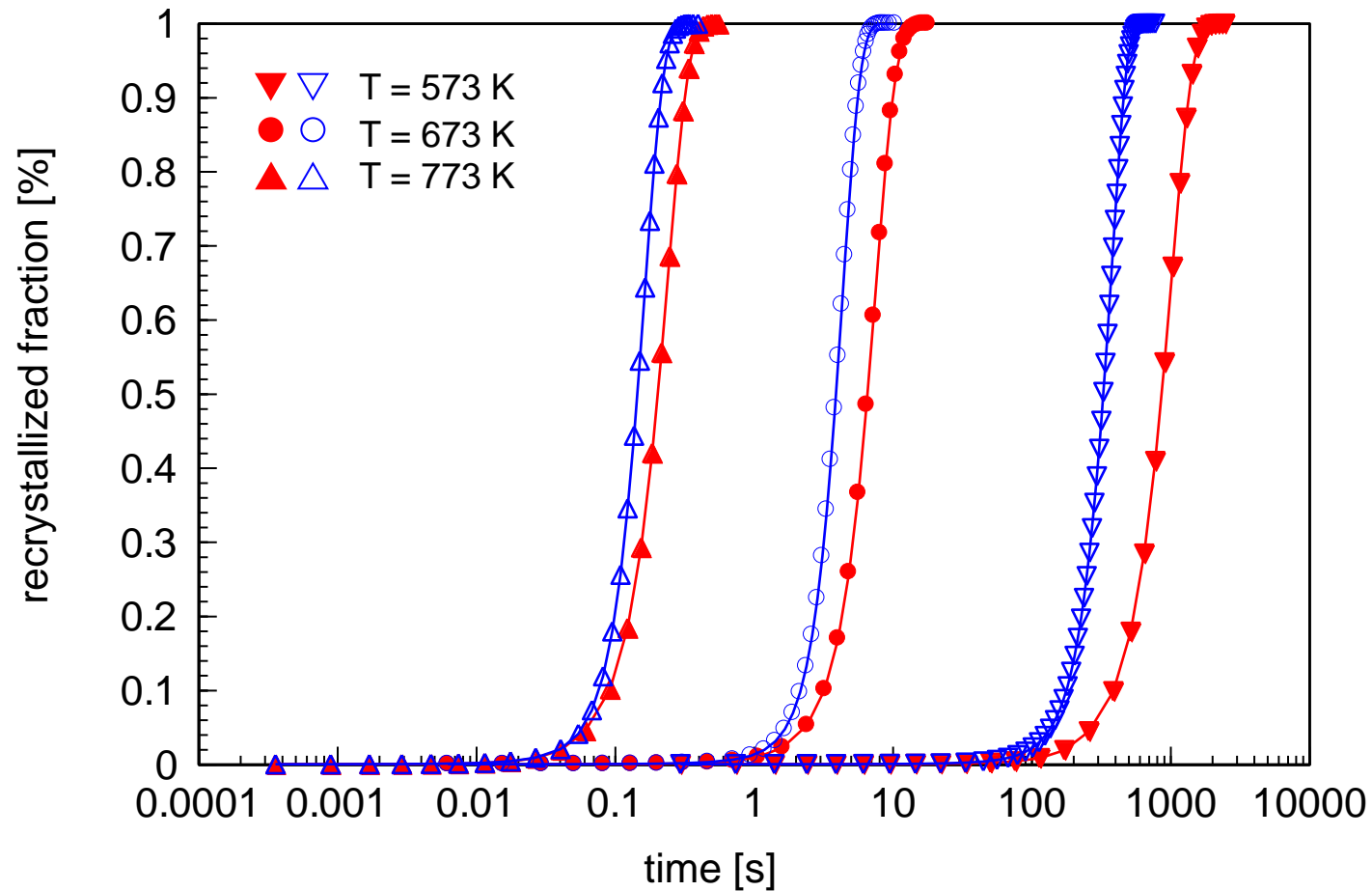
Initial fraction of LAGB in nucleus distribution: ~4.9%



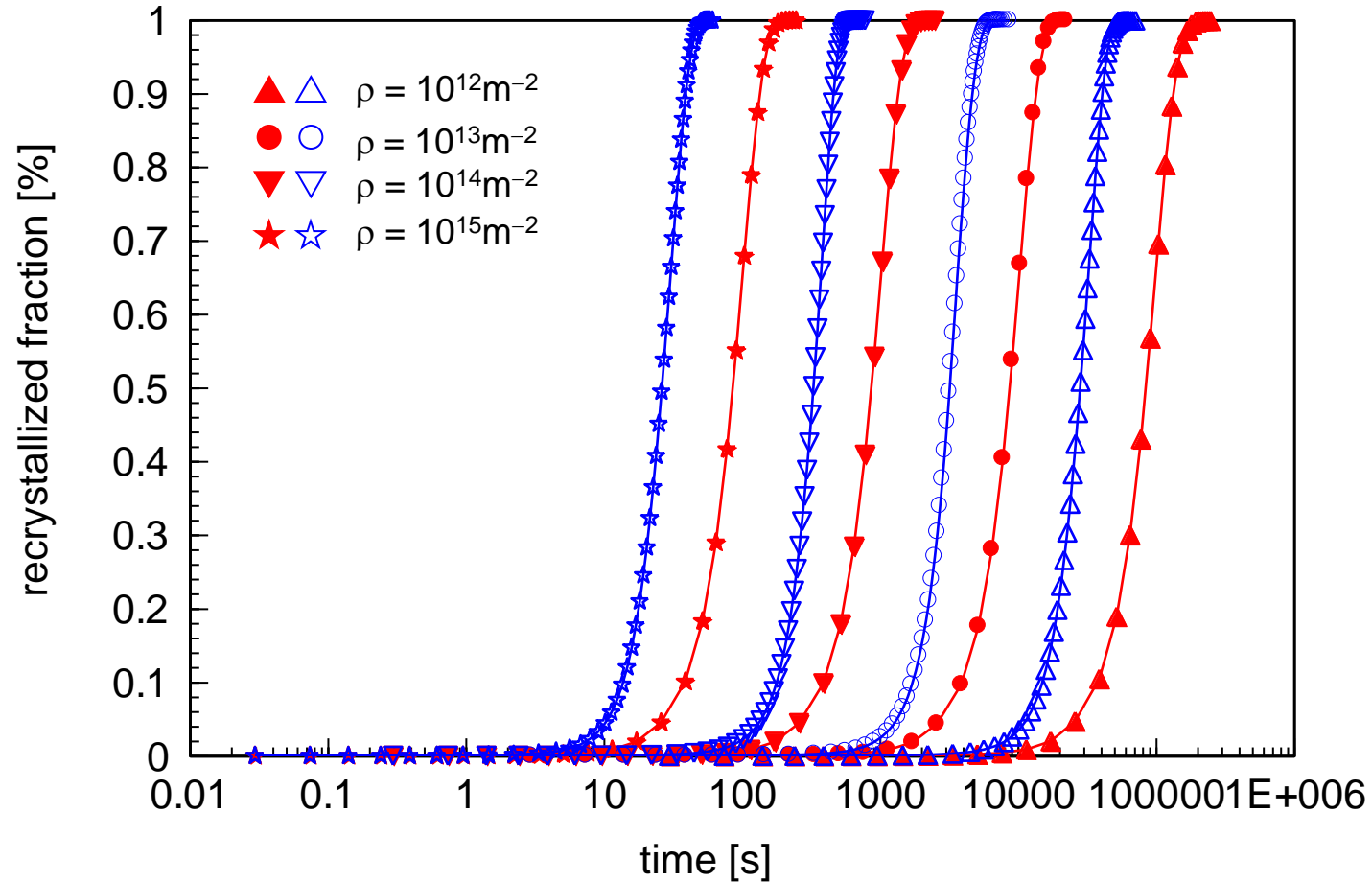
Influence of mobility for constant dislocation density $\rho=10^{14} \text{ m}^{-2}$, number of nuclei $w=0.05\%$ and temperature $T=573 \text{ K}$.



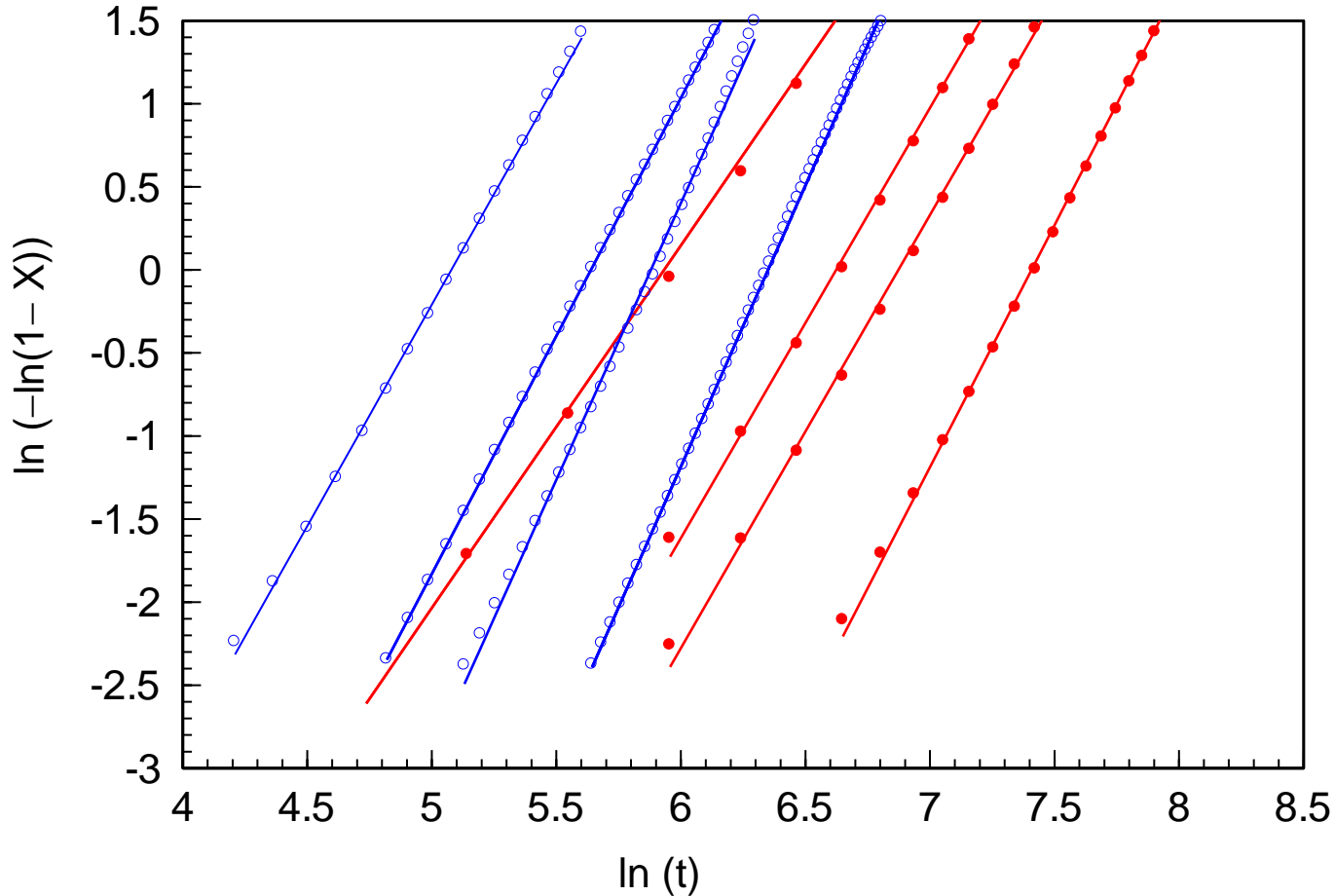
Influence of number of nuclei for constant dislocation density $\rho=10^{14}\text{m}^{-2}$ and temperature $T=573\text{K}$.



Influence of temperature for constant dislocation density $\rho=10^{14}\text{m}^{-2}$ and number of nuclei $w=0.05\%$.



Influence of dislocation density for constant number of nuclei $w=0.05\%$ and temperature $T=573\text{K}$.



Determination of Avrami exponent q from Avrami plot based on:

$$\ln(-\ln(1-X)) = q \cdot \ln t + \ln k_0$$

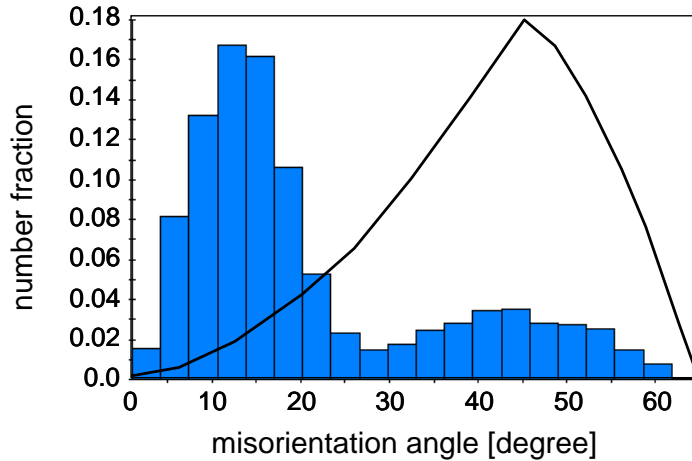
Mobile LAGB and HAGB	Only mobile HAGB
$\rho=10^{14} \text{m}^{-2}; T=573\text{K}; w=0.01\%; \mathbf{q=3.30}$	$\rho=10^{14} \text{m}^{-2}; T=573\text{K}; w=0.01\%; \mathbf{q=2.91}$
$\rho=10^{14} \text{m}^{-2}; T=573\text{K}; w=0.05\%; \mathbf{q=3.30}$	$\rho=10^{14} \text{m}^{-2}; T=573\text{K}; w=0.05\%; \mathbf{q=2.74}$
$\rho=10^{14} \text{m}^{-2}; T=573\text{K}; w=0.1\%; \mathbf{q=2.89}$	$\rho=10^{14} \text{m}^{-2}; T=573\text{K}; w=0.1\%; \mathbf{q=2.74}$
$\rho=10^{14} \text{m}^{-2}; T=573\text{K}; w=0.5\%; \mathbf{q=2.72}$	$\rho=10^{14} \text{m}^{-2}; T=573\text{K}; w=0.5\%; \mathbf{q=2.68}$
$\rho=10^{14} \text{m}^{-2}; T=673\text{K}; w=0.05\%; \mathbf{q=2.82}$	$\rho=10^{14} \text{m}^{-2}; T=673\text{K}; w=0.05\%; \mathbf{q=2.75}$
$\rho=10^{14} \text{m}^{-2}; T=773\text{K}; w=0.05\%; \mathbf{q=3.09}$	$\rho=10^{14} \text{m}^{-2}; T=773\text{K}; w=0.05\%; \mathbf{q=2.70}$
$\rho=10^{12} \text{m}^{-2}; T=573\text{K}; w=0.05\%; \mathbf{q=3.28}$	$\rho=10^{12} \text{m}^{-2}; T=573\text{K}; w=0.05\%; \mathbf{q=2.68}$
$\rho=10^{13} \text{m}^{-2}; T=573\text{K}; w=0.05\%; \mathbf{q=3.17}$	$\rho=10^{13} \text{m}^{-2}; T=573\text{K}; w=0.05\%; \mathbf{q=2.79}$
$\rho=10^{15} \text{m}^{-2}; T=573\text{K}; w=0.05\%; \mathbf{q=3.21}$	$\rho=10^{15} \text{m}^{-2}; T=573\text{K}; w=0.05\%; \mathbf{q=2.75}$

$>q_{\text{theo}}=3$ site saturated nucleation
but different growing rates

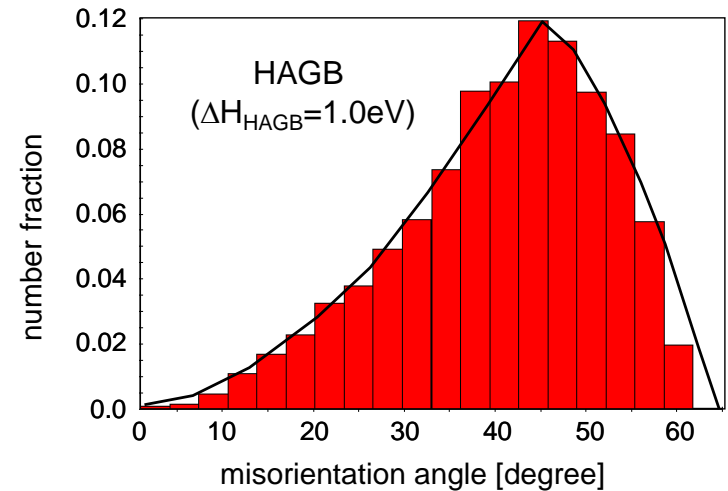
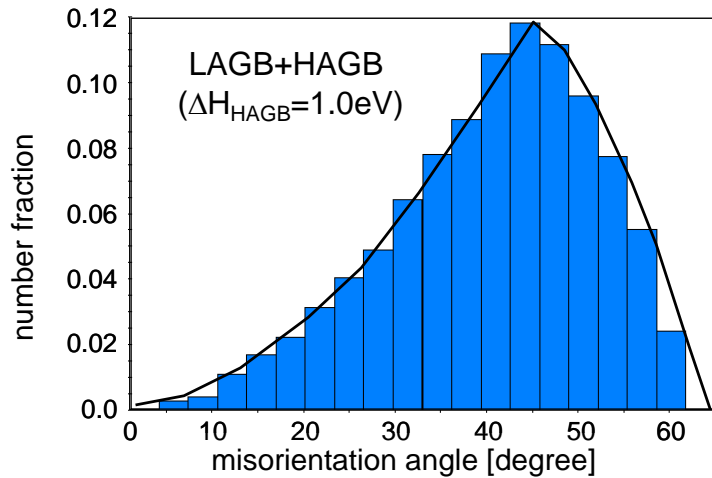
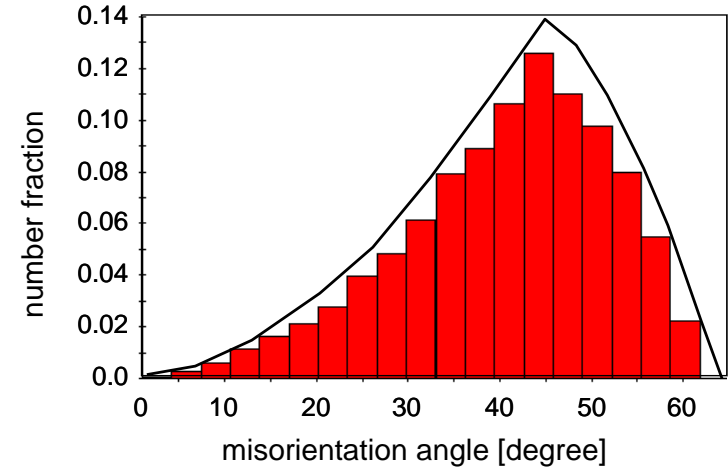
$\sim q_{\text{theo}}=3$ site saturated nucleation
and constant growing rate

Obviously, recrystallization in LAGB case is much faster than recrystallization in HAGB case.

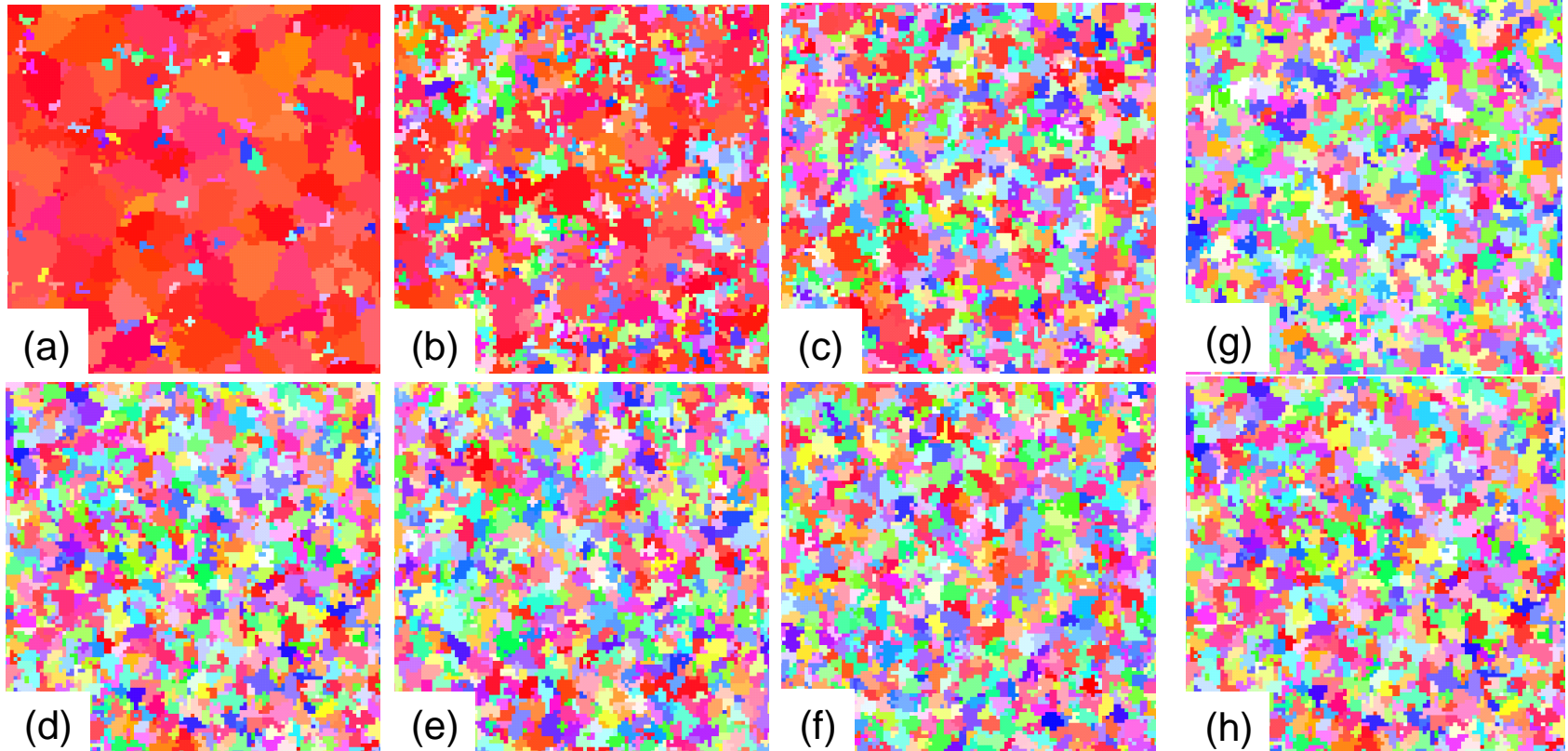
LAGB+HAGB
($\Delta H_{\text{HAGB}}=1.6\text{eV}$)



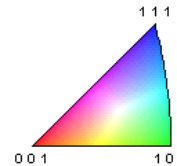
HAGB
($\Delta H_{\text{HAGB}}=1.6\text{eV}$)



Initial dislocation density for these simulations: $\rho=10^{14}\text{m}^{-2}$, number of nuclei $w=0.05\%$ and $T=573\text{K}$. The Mackenzie distribution is plotted as solid line and gives the distribution for a completely random



50μm

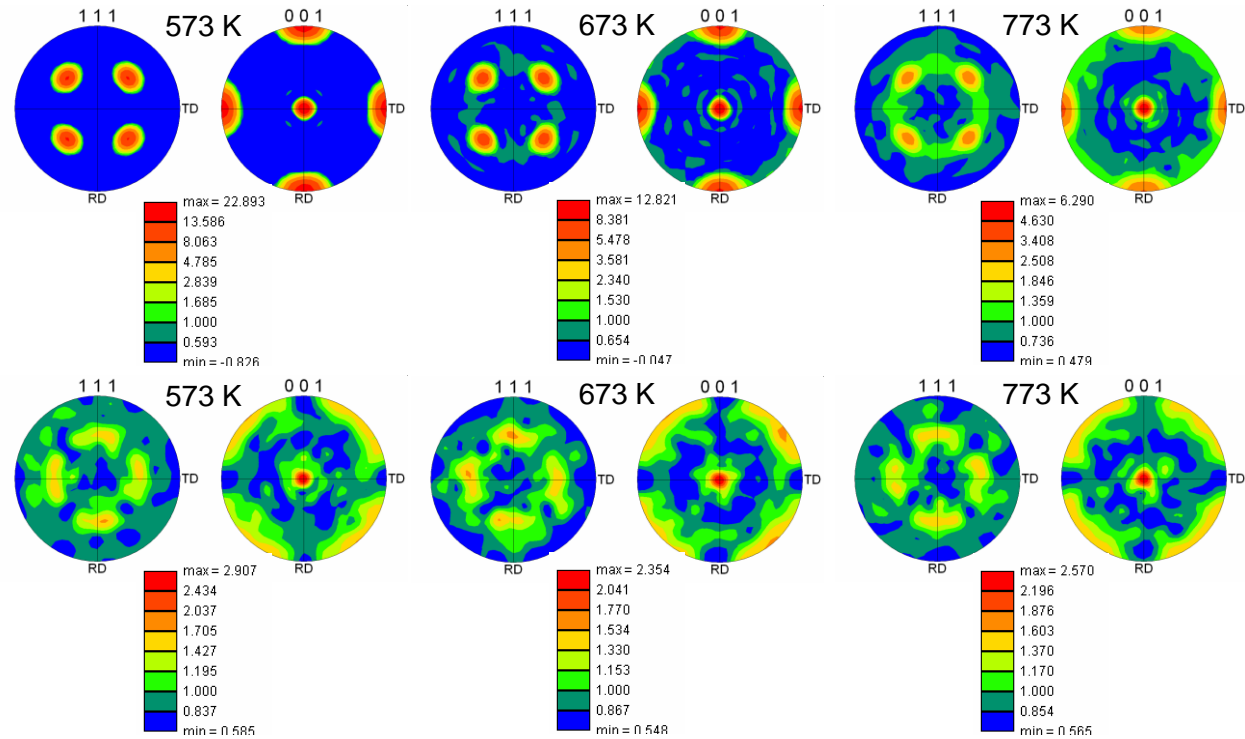


$w=0.05\%$ and $\rho=10^{14}\text{m}^{-2}$

(a) $m_{\text{LAGB}} > 0$ and $m_{\text{HAGB}} > 0$ at 573 K. (b) $m_{\text{LAGB}} > 0$ and $m_{\text{HAGB}} > 0$ at 673 K. (c) $m_{\text{LAGB}} > 0$ and $m_{\text{HAGB}} > 0$ at 773 K.

(d) $m_{\text{LAGB}} = 0$ and $m_{\text{HAGB}} > 0$ at 573 K. (e) $m_{\text{LAGB}} = 0$ and $m_{\text{HAGB}} > 0$ at 673 K. (f) $m_{\text{LAGB}} = 0$ and $m_{\text{HAGB}} > 0$ at 773 K.

At $T=573$ K: (g) $\Delta H_{\text{LAGB}}/\Delta H_{\text{HAGB}}=1.3\text{eV}/1.0\text{eV}$. (h) $m_{\text{LAGB}}=0$ and $\Delta H_{\text{HAGB}}=1.0\text{eV}$.

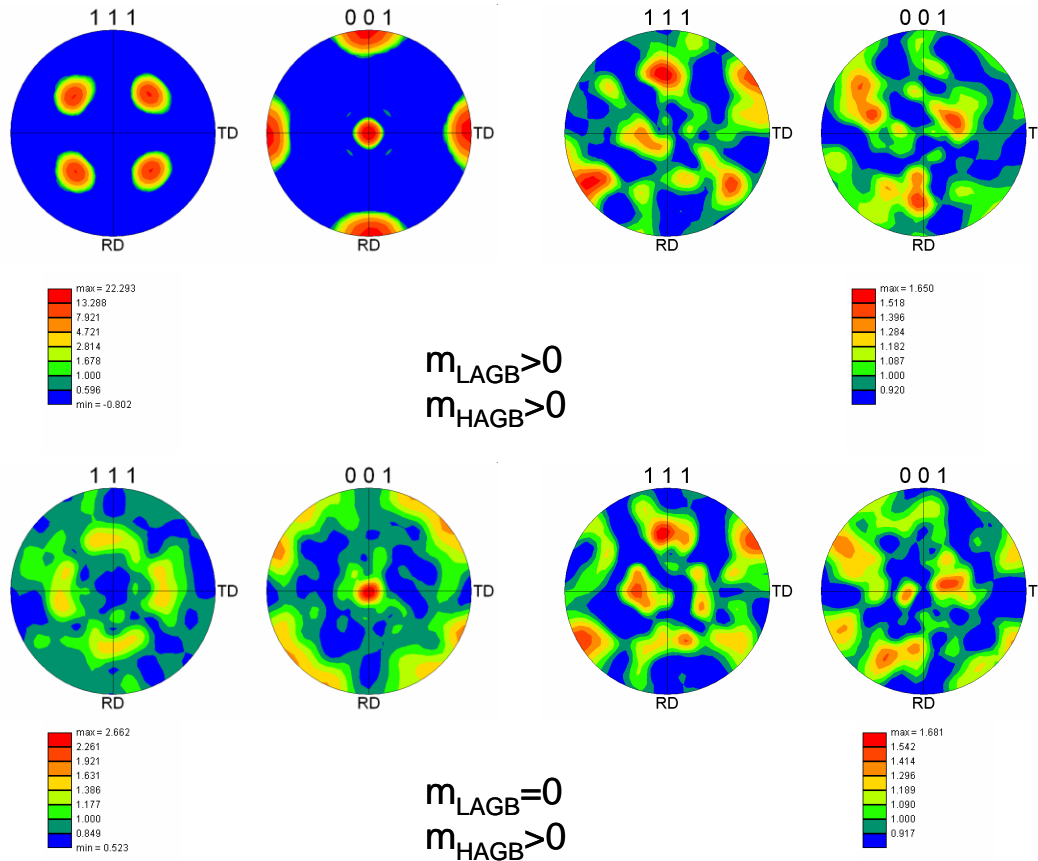


Pole figures for fully recrystallized Al single crystals with initial Cube orientation and $w=2\%$.

Upper row: Predicted textures at different temperatures for the case of mobile low and high angle grain boundaries:

Bottom row: Predicted textures at different temperatures for the case with only mobile high angle grain boundaries.

Initial dislocation density: $\rho=10^{14}\text{m}^{-2}$.



Upper row: Predicted textures for the cases of mobile low and high angle grain boundaries:
 Left side: $\Delta H_{LAGB}/\Delta H_{HAGB}=1.3\text{eV}/1.6\text{eV}$; right side: $\Delta H_{LAGB}/\Delta H_{HAGB}=1.3\text{eV}/1.0\text{eV}$.

Bottom row: Predicted textures for the cases with only mobile high angle grain boundaries.
 Left side: $m_{LAGB}=0$ and $\Delta H_{HAGB}=1.6\text{eV}$; right side: $m_{LAGB}=0$ and $\Delta H_{HAGB}=1.0\text{eV}$.

Initial dislocation density for these simulations: $\rho=10^{14}\text{m}^{-2}$, number of nuclei $w=0.05\%$ and $T=573\text{K}$.



- Results of 3D cellular automaton simulations were shown. Three cases were compared in order to study the influence of mobile low angle grain boundaries on the recrystallization behavior.
- The texture evolution shows an increasing randomization for the HAGB simulations. For LAGB simulations the texture remains stable up to 100% recrystallized fraction.
- The kinetics of recrystallization is faster for the LAGB simulations than for the HAGB simulations.
- The fraction of low angle grain boundaries is remarkably larger in the LAGB simulation case.
- The presented simulation results show that there is obviously an influence of low angle grain boundaries on the texture evolution during recrystallization.
- Further simulations are needed in order to get data which can be compared with experimental results.



Funding:
MPG, DFG